

## ACCOUNTING FOR SUB-HOURLY IRRADIANCE FLUCTUATIONS IN HOURLY PERFORMANCE SIMULATIONS

Michele Oliosi, Bruno Wittmer, André Mermoud, Agnes Bridel-Bertomeu  
PVsyst SA  
Route de la Maison-Carrée 30 - 1242 Satigny – Switzerland, [support@pvsyst.com](mailto:support@pvsyst.com)

**ABSTRACT:** Hourly performance simulations tend to report higher yields than sub-hourly performance simulations. One reason is that the clipping losses due to sub-hourly irradiance fluctuations will be underestimated in hourly simulations. In a previous work [1], we developed a model to estimate these extra clipping losses; it can be used to remove most of the yearly discrepancy between minute-level and hourly results.

In this work we show how part of the remaining yearly discrepancies are an artefact from applying transposition models at the sub-hourly level. Taking as example the widely used Perez model, we propose a way to correct the diffuse decomposition coefficients in the minute simulation, which further reconciliates hourly- and minute-level simulations.

**Keywords:** Simulation, System Performance, Subhourly, Irradiance, Clipping

### 1 MOTIVATION

Hourly simulations are widely used to estimate the performance of PV systems at different stages of their development and operation. While simulations using shorter time scales are also possible and used in some instances, hourly simulations have the advantage of having a shorter simulation time, and a wide availability of data, since hourly weather data is easier to collect.

However, weather, and in particular irradiance, may also exhibit important sub-hourly fluctuations. The effects of these fluctuations are therefore not necessarily well captured by hourly simulations. As several studies (see references collected in [1]) have shown, using hourly data leads on average to overestimating yearly yields by up to a few percent. This mostly depends on the DC:AC ratio of the system, in addition to the details of the sub-hourly weather data.

Indeed, for higher DC:AC ratios, sub-hourly fluctuations of the weather may drive momentarily the DC output across the threshold for inverter clipping. When simulating in hourly time steps, these sudden drops or peaks in the DC production may be missed. This results in missing clipping losses in the hourly simulation. After accumulating the missed clipping losses over a full simulation, the yearly performance may then be overestimated by a few percent. This makes it one, if not the main cause for the discrepancy between hourly and sub-hourly simulations.

In a previous study [1], we have presented a model that estimates the missing clipping losses at each hour, based on 3 hourly parameters fitted from the input horizontal-plane minute global irradiance data. The advantage of this method is that the simulation may be then run in hourly steps, thus keeping a lower overall simulation time, while reasonably modeling the missed clipping losses.

After correcting the clipping losses, however, there remained a bias towards higher yields in hourly simulations. The remaining discrepancies are shown in Figure 1 for different DC:AC ratios, but usually remain below the percent level.

In this paper, after first explaining our methodology in Section 2, we show in Section 3 that the remaining discrepancy is partially attributable to applying certain transposition models to the minute data. This implies that by applying these same transposition models to minute data, the minute-level simulations, previously used as a reference, may be biased towards underestimating the

yield of the system. We then investigate how the discrepancy between minute-level and hourly transposition is generated. We identify the non-linearity of certain transposition steps as the main cause for the averaging error.

Based on this observation we then propose in Section 4 a simple method to calculate new coefficients to be used within the widely used Perez model when applied to minute data. The method itself may be straightforwardly applied to wider datasets than the one used in this paper and may be also adapted to other coefficient-based models. We then discuss the results and conclude in Section 5.

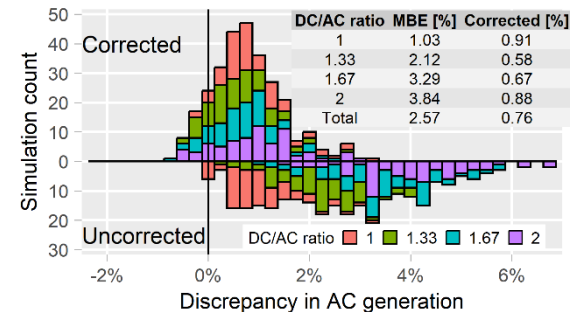


**Figure 1:** Histograms for the discrepancies in AC generation, across all simulated cases (4 DC:AC ratios, 18 orientations, 4 sites). Different DC:AC cases are highlighted in different colors. The transposition model is the Perez 1990 model [2]. Positive counts have had their clipping losses corrected with the model [1], negative counts are uncorrected.

### 2 METHODOLOGY

With the goal of achieving a better understanding of how the discrepancies are generated throughout the simulation process, and especially at the transposition step we reanalyze the same dataset that was studied in [1], and complement it with new results.

#### 2.1 Input and system data

We use as input data the minute-level measurements of global horizontal (GHI) and diffuse horizontal (DHI) irradiances, from four stations in the U.S. listed by the NREL Measurement and Instrumentation Data Center (MIDC). These are the NREL SRRL Baseline

Measurement System [3], in Golden, Colorado (abbreviated NRELSRRL); the University of Oregon [4], in Eugene, Oregon (abbreviated UniOregon); the Natural Energy Laboratory of Hawaii Authority [5], in Kailua-Kona, Hawaii (abbreviated Hawaii); and the University of Louisiana at Lafayette [6], in Lafayette, Louisiana (abbreviated Lafayette). These four sites belong to four different Köppen climate classes: respectively, semi-arid continental (BSk), warm-summer Mediterranean (Csb), tropical semi-arid (BSh), and humid subtropical (Cfa). The year considered is 2020 for all results, except the determination of new Perez coefficients in Section 4, for which we have used 2018, 2019, 2020 for NRELSRRL and UniOregon and 2019 and 2020 for Hawaii and Lafayette.

As PV systems, we consider four different DC:AC ratios (1, 1.33, 1.67, 2) and the seventeen fixed orientations of [1], and an additional single-axis tracker orientation. The inverter nominal power is fixed at 9kVA, and the DC:AC ratio is varied by considering different number of PV module strings. When averaging over multiple scenarios or climates, we have given the same weight to all cases.

## 2.2 Simulation procedure

For both minute-level and hourly simulations, we use PVsyst version 7.4.0. The hourly simulation is handled natively by the software, but the minute-level simulation is performed using the procedure described in [1]. This procedure works on the premise of combining 60 hourly simulations to mimic a single minute-level simulation. For the minute simulations, the array temperature is assumed to be stable during each hour. To obtain the value for the array temperature for the minute simulations, we use the hourly simulation results. Finally, most, albeit not all, output variables are available in the release version of the software.

## 2.3 Transposition models

The default transposition model used in PVsyst is the Perez 1990 model [2], which we abbreviate here “Perez model” for simplicity. The base for this model is the decomposition of the horizontal irradiance into different components, denoting different sky sectors: direct, circumsolar, and isotropic diffuse. In addition to these, the horizon band component, which is not measurable in the horizontal plane, is estimated from the horizontal irradiances.

The decomposition and estimation of the components on the horizontal (or vertical) plane follows simple equations,

$$\begin{aligned} \text{direct} &= \text{GHI} - \text{DHI} , \\ \text{isotropic diffuse} &= (1 - F_1) \text{DHI} , \\ \text{circumsolar} &= F_1 \text{DHI} , \\ \text{horizon band} &= F_2 \text{DHI} , \end{aligned}$$

where  $F_1$  and  $F_2$  are determined from

$$\begin{aligned} F_1 &= F_{11}(\epsilon) + F_{12}(\epsilon) \Delta + F_{13}(\epsilon) Z , \\ F_2 &= F_{21}(\epsilon) + F_{22}(\epsilon) \Delta + F_{23}(\epsilon) Z , \end{aligned}$$

where  $\Delta$  denotes the sky brightness,  $Z$  the sun zenith angle,  $\epsilon$  the sky clearness, and where the 6 factors  $F_{ij}(\epsilon)$  have values over 8 clearness bins, in total 48 numeric coefficients. In the 1990 publication [2], these coefficients

have been fitted with hourly and 15-minute measurements. The definitions for sky brightness and sky clearness are to be found in the same article.

The Hay-Davies model [7] (which we abbreviate “Hay model” in certain parts of the text) is simpler, in that it does not consider a horizon brightening band. Starting from the direct normal irradiance DNI and the extraterrestrial irradiance  $G_{ext}$  it defines an anisotropy factor  $A_i = \text{DNI}/G_{ext}$ , which is used to separate the horizontal diffuse irradiance into the isotropic and circumsolar parts,

$$\begin{aligned} \text{direct} &= \text{GHI} - \text{DHI} , \\ \text{isotropic diffuse} &= (1 - A_i) \text{DHI} , \\ \text{circumsolar} &= A_i \text{DHI} . \end{aligned}$$

We use the Hay-Davies model in section 3.3 to illustrate the impact of the transposition model on the discrepancy between minute-level and hourly data.

In both the Perez and Hay-Davies, the multiplicative transposition factors used to go from horizontal and vertical-plane irradiances to the plane of array are the same, i.e.,

$$\begin{aligned} \text{direct} &: \frac{\max(0, \cos \alpha)}{\cos Z} \\ \text{circumsolar} &: \frac{\max(0, \cos \alpha)}{\max(\cos 85^\circ, \cos Z)} \\ \text{isotropic diffuse} &: \frac{1 + \cos \theta}{2} \\ \text{horizon band} &: \sin \theta \end{aligned}$$

where  $\alpha$  is the incidence angle between the normal to the plane of array and the sun direction,  $Z$  the zenith angle, and  $\theta$  the tilt of the plane of array.

Both models are implemented in PVsyst making it possible to run PV performance simulations with either of these.

## 3 TRANSPOSITION DISCREPANCIES

### 3.1 Propagation of the discrepancy

The discrepancy between hourly and minute-level simulations can be evaluated at different stages of the simulation process. The good correlation between the discrepancies at the transposition, DC energy, and AC energy evaluation stages for all simulation cases, can be considered as strong evidence for the importance of the transposition stage in the generation of the discrepancies. We summarize the results at the different stages in Figure 2, where we illustrate by a linear fit the correlation of the discrepancies. A better fit is achieved between the transposition stage and the DC energy evaluation stage. Denoting as  $b_{E_{AC}}$ ,  $b_{E_{DC}}$ ,  $b_{G_{\text{GlobInc}}}$  the yearly relative discrepancy in AC energy, DC energy, and transposed irradiance respectively, we find the following fits:

$$\begin{aligned} b_{E_{DC}} &= 1.01 b_{G_{\text{GlobInc}}} , & \sigma &= 0.07\% , & R^2 &= 0.99 , \\ b_{E_{AC}} &= 0.77 b_{G_{\text{GlobInc}}} , & \sigma &= 0.47\% , & R^2 &= 0.57 , \end{aligned}$$

The latter fit, i.e. between the discrepancy at the AC stage and at the transposition stage, shows that despite the clipping correction model, a certain discrepancy is still generated by the DC to AC conversion model. Note that these fits are specific to the set of simulations chosen, and may be different for a different set of simulations. We

therefore interpret them qualitatively, without investigating the detailed values.

The average discrepancy across the simulations at the 3 stages is reported in Table 1. As we will show in Sections 3.2 and 4, it is possible to reduce the AC power discrepancy to about 0.5% on average, either by choosing another transposition scheme for both minute-level and hourly simulation, or by adapting the transposition model when it is applied to the minute-level data.

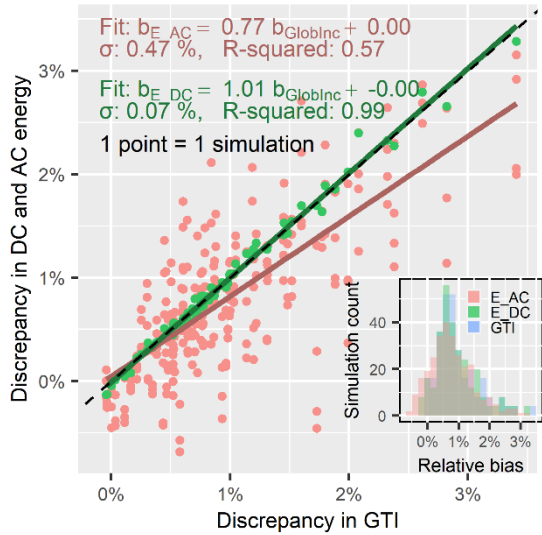


**Figure 2:** Correlation between the discrepancy in the global transposed irradiance (GTI), in blue in the histogram, and the discrepancies in the DC energy (green) and AC energy (red). Each point represents one simulation. Linear fits have been added to each series of points, they reflect the propagation of the discrepancy throughout the simulation.

**Table 1:** Average discrepancy across simulations for three different simulation stages.

Stage	Mean discrepancy	Std dev.
GTI	0.96 %	0.69 %
DC energy	0.95 %	0.71 %
AC energy	0.78 %	0.71 %

### 3.2 Transposition model comparison

Since the transposition of the irradiance components already leads to differences between the minute-level and hourly simulation, it is natural that the choice of the transposition model will have an impact on the discrepancy. To illustrate this, we run the same set of simulations but using the Hay transposition model instead of the Perez transposition model. The Hay transposition model is chosen for this comparison because it is simpler than the Perez model, leading to a smaller chance of accumulating averaging errors.

The comparison of the yearly results from the two transposition models is shown in Figure 3. The mean values and overall behavior of the histogram show that the Hay model in general will have less discrepancies.

In Figure 4, we show the discrepancies by site, and discriminating between irradiance components, in addition to showing the GTI values only. Indeed, the Hay transposition handles the direct component in the same

way as the Perez transposition. Differences therefore show up rather in the handling of the diffuse.

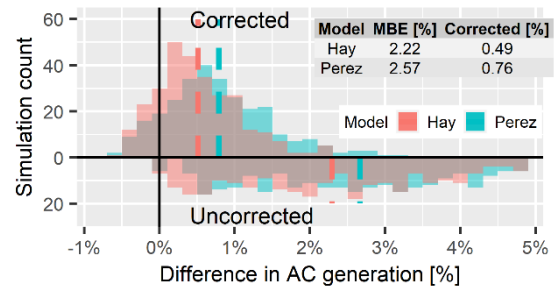


**Figure 3:** Histograms for the discrepancies in AC generation, across all simulated cases. We use two transposition models, the Perez 1990 model [2] in blue, and the Hay-Davies mode [7] in red. Positive counts have had their clipping losses corrected with the model [1], negative counts are uncorrected. See Figure 1 for the Perez data with a breakdown of the DC:AC cases.

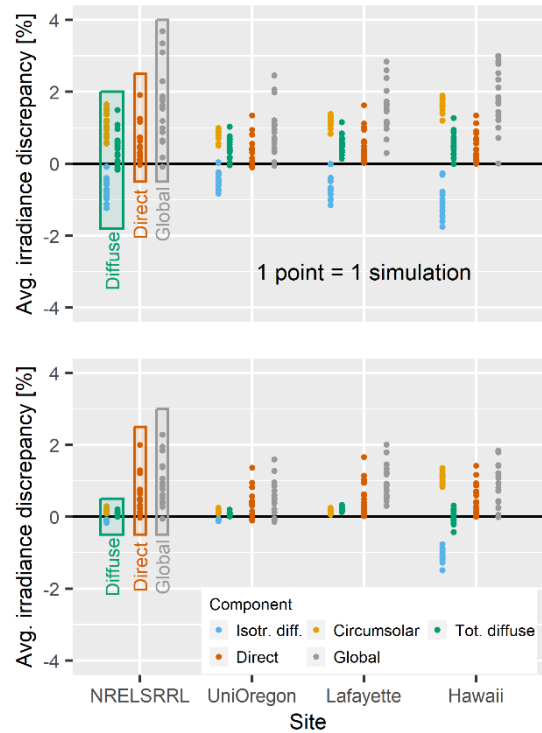


**Figure 4:** Site by site breakdown of the average transposed irradiance discrepancies, by simulation. We separate the different irradiance components: the global in grey, is composed by the sum of direct (orange) and diffuse irradiances (green). The diffuse can be further reduced to the sum of circumsolar (yellow) and isotropic diffuse (blue), which includes here the horizon band component.

It is however interesting to note that for both the Hay and Perez model, the transposition of the direct component generates a sizeable part of the discrepancy, however less so at common orientations such as 30°-South. This is illustrated further in Figure 5, in which we show the discrepancies in the transposed direct component as a function of the azimuth and tilt. We interpret the direct component transposition procedure as an instantaneous procedure, because it entirely depends on geometric

variables such as the sun position. It is therefore preferentially applicable to shorter time scales, for which these variables vary less within a time step. Therefore, the transposition of the direct component should be corrected in the hourly simulations.

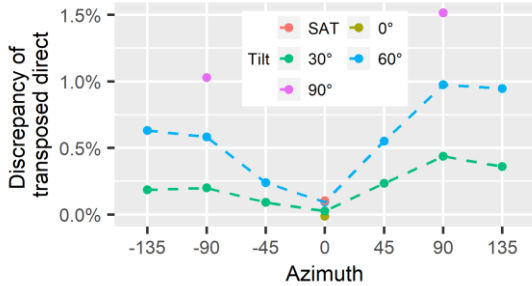


**Figure 5:** Discrepancies generated at the transposition of the direct irradiance component, as a function of the azimuth, and colored by tilt. The case of a single North-South-axis tracker (SAT) is shown in red. Typical south-facing orientations are the least affected by this type of transposition bias. In this case, we interpret the minute values as the reference, i.e. the hourly values need to be corrected.

Regarding the diffuse components, the sum of isotropic diffuse and circumsolar components produces a negligible discrepancy in the Hay model. These two components themselves have negligible discrepancies for all sites except Hawaii. Contrary to the Hay model, the Perez transposition, has a sizeable discrepancy in the diffuse components roughly of the same magnitude as the direct component.

It is instructive to visualize the differences between components when averaging discrepancies separately over each hour of the day. We show this in Figure 7, by choosing a specific site, year, and selecting the 30°-South orientation. By doing so, one can visually identify the difference between direct and diffuse irradiances. The direct irradiance generates a pronounced discrepancy around sunrise and sunset exclusively. The reason for this is still unclear to us, but this may be related either to the handling of the sun crossing the horizon line, or to the fact that at these hours the incidence angle and transposition factor change more drastically than in the middle of the day, for a typical equator-facing orientation.

In the Perez model, the discrepancies for the horizontal decomposed diffuse components are already quite marked. However, due to how the decomposition of circumsolar and isotropic diffuse is defined, the respective discrepancies compensate each other. However, because the geometrical transposition factor given in Section 2.3 is different for each component, once these have been transposed the isotropic diffuse and circumsolar discrepancies do not compensate each other any more on the plane of array. The horizon band generates a discrepancy already present in the vertical plane. It is not compensated by other factors therefore it remains present once transposed to the plane of array. The Hay model, with example profiles shown in Figure 8, generates negligible discrepancies for the diffuse components in the horizontal plane. Once the transposition factors are applied, the discrepancies remain small.

To summarize, the discrepancy in the diffuse components appears, already at the level of the

decomposition into horizontal (and vertical) contributions. This is dependent on the specific transposition model and is more prevalent in the Perez model with respect to the Hay model. The transposition to the plane of array simply exacerbates their impact. The discrepancy of the direct component appears when transposing in the plane of array in both models. This suggests that it depends mainly on the orientation, and does not depend on the transposition model. This further suggests that the transposed direct irradiances are more accurate when considering minute-level data.

## 4 PEREZ-MINUTE COEFFICIENTS

### 4.1 Correction philosophy

As seen in the previous section, the transposed diffuse irradiance averaging errors originate mainly from the diffuse decomposition into horizontal and vertical components. The latter non-linear step is at the core of the Perez model. While the detailed mechanism of the generation of a bias via the individual averaging errors is still elusive, it seems inevitable that differences will arise between the minute-level and hourly data transpositions, because of the non-linearities involved.

The model [2] has originally been built using hourly and 15-minute irradiance measurements, with the aim of reproducing the observed plane of array irradiance values. Therefore, when comparing the two sets (minute-level and hourly transposed data) it seems justified to use the hourly transposed values as a reference, since this is the experimentally verified case. This raises the question of whether a correction of the transposition process for minutes could be achieved, with the goal of bringing the hourly and minute results closer to each other, and especially to remove the bias component of the discrepancy.

In what follows we suggest a way to correct the minute transposition via a new set of coefficients  $F_{ij}(\epsilon)$ , computed using the hourly transposed values as a reference. Schematically, the procedure is depicted in Figure 6. This is of course one among many possible correction methodologies, but it has the advantage of not modifying the model fundamentally, but rather to adjust a few numeric coefficients while retaining the qualitative aspects of the model. We further note that the fitting of coefficients in the Perez model is a common practice suggested in [2], for example to determine coefficients specific to a given climate or region (see e.g. [8] or [9]).

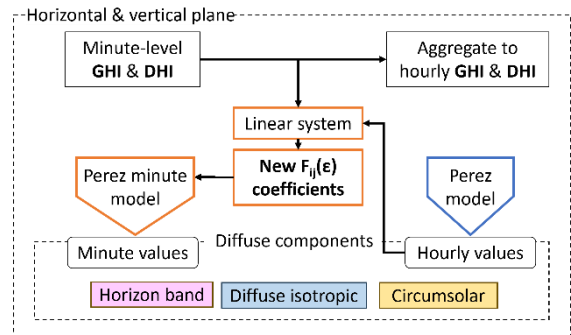


**Figure 6:** Scheme of the generation method for new Perez coefficients, to be used with minute data and fitted to minimize the mean square differences with the hourly diffuse decomposition determined with the original

coefficients.



**Figure 7:** Daily profile of the discrepancies for different irradiance components with the Perez transposition. An average for the whole simulation by hour of the day has been taken. Once transposed, components that compensated each other in the horizontal plane now generate a bias.

#### 4.2 Perez coefficient fitting

For each hour, the difference between the minute level and the hourly estimate of the horizontal circumsolar irradiance is given by  $\langle F_1 \text{DHI} \rangle_H - F_{1H} \langle \text{DHI} \rangle_H$ , where  $H$  denotes a given hour in the dataset, and  $\langle \rangle_H$  is an average over that hour. An equivalent form can be written for  $F_2$  for the vertical-plane horizon band irradiance component. We choose as best fit the one that will minimize the mean-square of these differences. It is possible to add weight filters to the individual hours. We choose to fit over data for which the  $\text{DHI} > 10 \text{ W/m}^2$ , to eliminate most night data, and choose an equal weight for all remaining hours. We accumulate the mean-square of the differences using data described in Section 2, including several years.

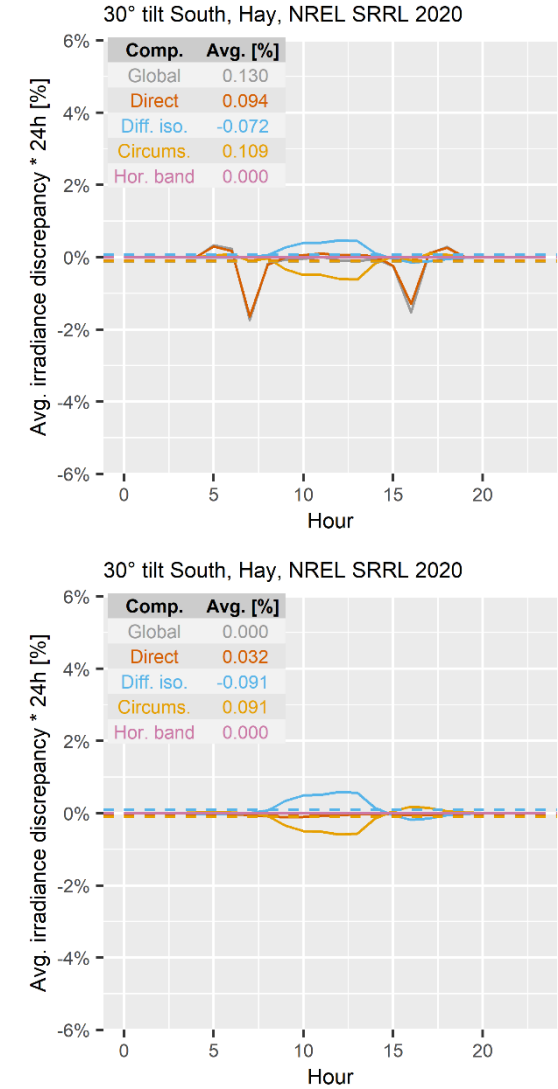


**Figure 8:** The same as Figure 7, but with the Hay model. Discrepancies are much less prevalent at the decomposition stage than with the Perez model. After transpositions, the discrepancies stay small.

The fitting procedure amounts to solving a pair of linear systems of equations,

$$\frac{\partial}{\partial F_{1jk}} \sum_{\text{sites}, H} (\langle F_1 \text{DHI} \rangle_H - F_{1H} \langle \text{DHI} \rangle_H)^2 = 0 ,$$

$$\frac{\partial}{\partial F_{2jk}} \sum_{\text{sites}, H} (\langle F_2 \text{DHI} \rangle_H - F_{2H} \langle \text{DHI} \rangle_H)^2 = 0 ,$$

for all  $j = 1, 2, 3$  and  $k = 1, \dots, 8$  the index denoting the clearness  $\epsilon$  bin, between values  $\epsilon = 1, 1.065, 1.23, 1.5, 1.95, 2.8, 4.5, 6.2, \text{ and } \infty$ . Indeed, formally it is possible to write

$$F_i = \sum_k \Pi_k(\epsilon) (F_{i1k} + F_{i2k} \Delta + F_{i3k} Z) ,$$

where  $\Pi_k$  is the Heaviside Pi function for bin  $k$ . Each of the 48  $F_{ijk}$  will be subject to the fitting procedure, leading

to a new set of 48  $F_{ijk}$  deviating from the original set in [2].

The result of the fitting procedure is summarized in Figure 9, and numerical coefficients are reported in Appendix A. Of course, applying this procedure to a wider minute-level dataset can provide more statistical significance to the fits. It is notable that the fitting procedure does not modify extensively the parameters, excepting central clearness bins for  $F_{12}$  and  $F_{22}$ .

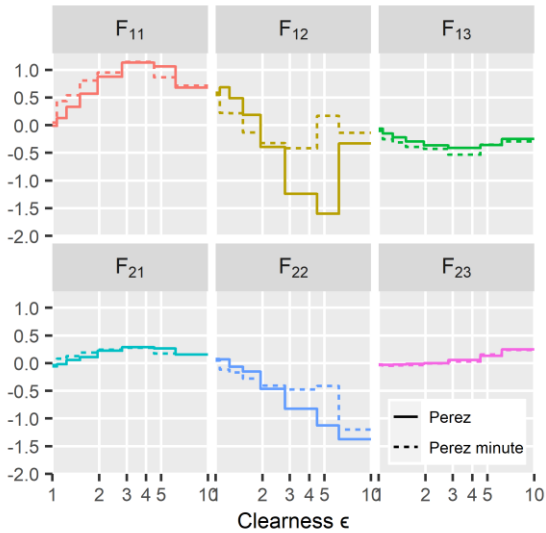


**Figure 9:** New Perez-minute coefficients, as obtained from the procedure in Figure 6, compared to the original 1990 publication ones [2], used for the hourly simulation.

#### 4.3 Procedure validation

In order to illustrate the impact of the new coefficient on the minute transposition, we reproduce Figures 7 and 8, i.e. aggregate the results for a specific site and one specific year, for each hour of the day, this time however after using the new Perez-minute coefficients for the minute level calculations. The result is depicted in Figure 10. The new transposition coefficients help achieving a much better agreement with the hourly Perez transposition results. Since the discrepancy is reduced already for horizontal irradiances and for the vertical-plane horizontal band irradiance, after applying the usual transposition factors, the discrepancy remains small of the order of 0.1% for the global irradiance.

Note that because of the mildly tilted and south-facing orientation, the impact of the direct irradiance transposition factor is small. For different orientations, the transposition factors may have a bigger impact. Overall, the discrepancies are expected to be comparable with the more linear Hay-Davies model, as in Figure 8.

## 6 DISCUSSION AND OUTLOOK

### 6.1 Summary

In this work, we have first complemented and reanalyzed the same data as in [1], i.e. minute-level and hourly simulation results based on four sites with different climates, a wide range of orientations, and four DC:AC ratios. Despite having corrected the hourly simulations for the missing clipping losses due to sub-hourly fluctuations,

the minute-level and hourly simulated AC energies still differ by on average 0.8% more for the hourly results.

In order to find the cause for this remaining bias, we have studied the propagation of the discrepancy at different stages of the simulation. We have found that the discrepancy is already largely present after the transposition of the irradiances, and that ulterior simulation steps do not add much to the average discrepancies.

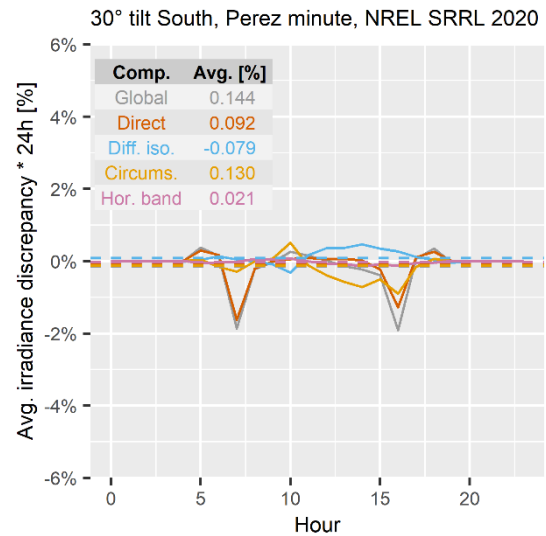
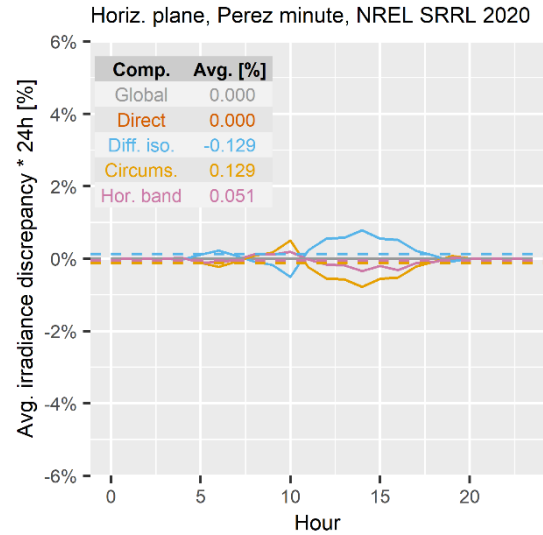


**Figure 10:** Daily profile of the discrepancies for different irradiance components with the new Perez minute coefficients used for the minute-level transposition. See Figure 7 for comparison with the Perez original coefficients.

By comparing the Perez and Hay transpositions, as well as decomposing the discrepancies into different irradiance components, we have recognized that two mechanisms cause significant discrepancies at the transposition stage: the geometric transposition of the direct component, and the horizontal and vertical-plane decomposition of the diffuse components, the latter effect being only prevalent in the Perez transposition model, due to the non-linear nature of the decomposition.

In order to address the issue of the discrepancy

generated by the separation of the diffuse components in the Perez model, we have proposed a method that allows to obtain a new set of 48 coefficients, based on minute-level horizontal global and diffuse irradiance data. These new coefficients allow to use the Perez model on minute-level data, and to recover transposed diffuse irradiances close to the respective hourly values. We applied the method on a limited set of data, with the intent of providing a proof of concept. The method should however be applied over larger datasets (including several climates, sites, and years) to gain in statistical significance.

## 6.2 Outlook

Based on this study, we recognize two directions in which this analysis can be improved, which will impact both minute-level and hourly simulations. First, it is important to address the discrepancies generated by the transposition of the direct irradiance. While for more typical south-facing orientations this effect is not so prevalent, this is critical for other common orientations, e.g. for vertical East-West bifacial arrangements. We believe that this should be addressed in the hourly simulations, since the direct transposition is by nature best applied over shorter time scales. Second, after correcting as much as possible for transposition effects, it should be possible to reanalyze the discrepancies related to clipping losses. As we have suggested in [1], there exists a wide range of different correction models for hourly simulations based on coefficients extracted from the minute data. The one studied in [1] is simple and efficient, but it could be improved.

In addition to these two directions, the exact mechanism behind the generation of a bias component from the Perez diffuse decomposition remains to be elucidated. Indeed, this could come among others from the non-linearity of the clearness determination, which depends for example on the zenith angle to the third power, from the binning in clearness, which could lead to jumps, or simply in the overall shape of the decomposition coefficients  $F_{ij}$  as functions of the clearness values.

## 7 REFERENCES

- [1] A. Viloz, B. Wittmer, A. Mermoud, M. Olios and A. Bridel-Bertomeu, "A Model Correcting the Effect of Sub-Hourly Irradiance Fluctuations on Overload Clipping Losses in Hourly Simulations," *8th World Conference on Photovoltaic Energy Conversion; 1151-1156*, 2022.
- [2] R. Perez, P. Ineichen, R. Seals, J. Michalsky and R. Stewart, "Modeling daylight availability and irradiance components from direct and global irradiance," *Solar Energy*, vol. 44, p. 271–289, 1990.
- [3] T. Stoffel and A. Andreas, *NREL Solar Radiation Research Laboratory (SRRL): Baseline Measurement System (BMS); Golden, Colorado (Data)*, Not Available, 1981.
- [4] F. Vignola and A. Andreas, *University of Oregon: GPS-based Precipitable Water Vapor (PWV)*, NREL-DATA (National Renewable Energy Laboratory - Data (NREL-DATA), Golden, CO (United States)), 2013.
- [5] K. Olson and A. Andreas, *Natural Energy Laboratory of Hawaii Authority (NELHA): Hawaii Ocean Science & Technology Park; Kailua-Kona, Hawaii*, NREL-DATA (National Renewable Energy Laboratory - Data (NREL-DATA), Golden, CO (United States)), 2012.
- [6] NREL, *University of Louisiana at Lafayette*, NREL-DATA (National Renewable Energy Laboratory - Data (NREL-DATA), Golden, CO (United States)).
- [7] J. E. Hay and J. A. Davies, "Calculations of the solar radiation incident on an inclined surface," *Proc. of First Canadian Solar Radiation Data Workshop*, 59. Ministry of Supply and Services, Canada., 1980.
- [8] D. Yang, Z. Ye, A. M. Nobre, H. Du, W. M. Walsh, L. I. Lim and T. Reindl, "Bidirectional irradiance transposition based on the Perez model," *Solar Energy*, vol. 110, p. 768–780, December 2014.
- [9] M. Meshkinkiya, R. C. G. M. Loonen, R. Paolini and J. L. M. Hensen, "Calibrating Perez Model Coefficients Using Subset Simulation," *IOP Conference Series: Materials Science and Engineering*, vol. 556, p. 012017, July 2019.
- [10] C. W. Hansen, J. S. Stein and D. Riley, "Effect of time scale on analysis of PV system performance," *SANDIA Report*, 2012.

## A NUMERICAL PEREZ-MINUTE COEFFICIENTS

We report in Table 2 the coefficients obtained by minimizing the mean-squared error between hourly horizontal and vertical-plane diffuse components (reference) and the respective minute-level values. The dataset used is described in Section 2.

**Table 2:** Legend

Clearness bin	$F_{11}$	$F_{12}$	$F_{13}$	$F_{21}$	$F_{22}$	$F_{23}$
[1-1.065)	0.0489	0.5429	-0.1035	-0.0356	0.0466	-0.0353
[1.065-1.23)	0.4339	0.2185	-0.2529	0.0814	-0.1142	-0.0462
[1.23-1.5)	0.5423	0.2124	-0.3100	0.1236	-0.1676	-0.0424
[1.5-1.95)	0.8067	-0.1334	-0.3941	0.1894	-0.2816	-0.0332
[1.95-2.8)	0.9534	-0.3256	-0.4268	0.2405	-0.4068	-0.0095
[2.8-4.5)	1.1437	-0.4193	-0.5341	0.2747	-0.4772	0.0262
[4.5-6.2)	0.8618	0.1698	-0.3524	0.1706	-0.4145	0.1544
[6.2-∞)	0.7136	-0.1367	-0.2966	0.1579	-1.1983	0.2392